ASPECTS OF FRACTURE MECHANICS IN CRYOGENIC MODEL DESIGN
PART I - FUNDAMENTALS OF FRACTURE MECHANICS

C. Michael Hudson
NASA Langley Research Center
Hampton, Virginia

This presentation provides a fundamental introduction to the use of fracture mechanics for predicting fracture and fatigue crack growth in metals. First, consider figure 1. The stresses (σ_y, σ_x, τ_{xy}) at any point in the vicinity of a crack tip can be defined in terms of three parameters. These parameters are (1) r, the distance from the crack tip to the point under consideration; (2) a function of δ, the angle between the x axis and r; and (3) K_I, the stress intensity factor. The term K_I is given by

$$K_I = S\sqrt{\pi a} \tag{1}$$

where S is the applied stress and a is one-half the length of the crack, for the following stress and configuration conditions:

1. A through-the-thickness crack
2. An infinite-width plate
3. A uniformly distributed stress

(Considerably more complex relationships apply for other configurations and stress conditions.)

When the failure process occurs under plane strain conditions, the value of K_{Ic} tends to remain constant for a given material and temperature. This constant value is defined as the plane strain fracture toughness of the material. For the specimen configuration shown in figure 2, K_{Ic} can be defined as

$$K_{Ic} = S\sqrt{\pi a_{critical}} \tag{2}$$

Once K_{Ic} has been determined, it can be used to predict the failure of cracked structures under plane strain conditions. (Considerably more complex procedures are required for predicting failure under plane stress conditions.) For example, if both K_{Ic} and the crack size have been determined for a certain component, the stress required to fail that component can be calculated. Similarly, the critical flaw size can be calculated if both K_{Ic} and the applied stress are known.

Many factors can affect the value of K_{Ic} for a given material. One of the most dominating factors is temperature. For many materials, the value of K_{Ic} drops precipitously with decreasing temperature. Figure 3 shows a generally linear drop in K_{Ic} with decreasing temperature for 18 Ni-(250) maraging steel (ref. 1). Figure 4 shows a rapid drop from approximately $-75^{\circ}F$ to $-200^{\circ}F$ (the transition temperature region), followed by a more gradual drop for temperatures below $-200^{\circ}F$ (ref. 1). (The data in figure 4 are from tests on A517 Grade F steel.) In both cases, the reduced values of K_{Ic} indicate that for a given stress condition, the critical flaw size decreases with decreasing temperature. This in turn indicates that greater care must be taken in inspecting structures for cryogenic applications.

Next, consider the fatigue crack growth aspects of fracture mechanics. Basic fatigue crack growth data can be generated using the center-cracked specimen shown in figure 5. This specimen is a flat sheet specimen containing a notch in the center. (Other specimen configurations are also used.) When this specimen is subjected to a cyclic loading, such as that shown in figure 6, a fatigue crack will initiate at the two ends of the notch. With continued cyclic loading, these cracks will grow towards the edges of the specimen. Figure 7 shows the variation of crack length against cycles for the loading condition shown in figure 6. The slope of

this fatigue crack growth curve at any point is defined as the fatigue crack growth rate, da/dN.

The stress intensity range ΔK can also be defined for any point on the fatigue crack growth curve. This stress intensity range is given by

$$\Delta K = \sqrt{\pi a}\ (S_{max} - S_{min}) \tag{3}$$

for the specimen in figure 5 when that specimen has an effectively infinite width. The terms S_{max} and S_{min} are defined in figure 6.

Once da/dN and ΔK have been calculated for a series of points along the fatigue crack growth curves, they can be plotted against each other, as shown in figure 8 (ref. 2). The correlation of these factors is quite good.

A relationship developed by Forman et al. (ref. 3) has been found to fit the plots of da/dN against ΔK quite well. This relationship is given by

$$da/dN = \frac{C\Delta K^n}{(1 - R)K_{Ic} - \Delta K} \tag{4}$$

for plane strain conditions. In equation (4), the terms C and n are empirical constants and R is defined by

$$R = S_{min}/S_{max} \tag{5}$$

This R term can have a significant effect on fatigue crack growth.

Figure 9 (ref. 2) shows plots of da/dN against ΔK for various R values. The data for a given R value fall into discrete scatterbands. However, the scatterbands for different R values are not coincident. Generally, the higher the R value for a given value of ΔK, the higher the rate of fatigue crack growth. Forman's equation (ref. 3) fit each of these scatterbands quite well with one coefficient and one exponent (See fig. 9.) Thus Forman's equation accounts for the R value effect quite well.

Once the coefficient and exponent have been determined, equation (4) can be numerically integrated to predict the life of cracked components. Figure 10 presents the results of one set of such predictions. For this set, the coefficient and exponent were calculated using data from tests on center-cracked specimens. Equation (4) was then used to predict the number of cycles required to grow surface cracks from their initial flaw sizes to failure (ref. 4). Tests were then conducted on specimens having these flaw sizes, and the actual fatigue lives were determined. Figure 10 shows the ratios of the tests lives to predicted lives. These ratios ranged from 0.51 to 1.84. Considering that the normal scatter in fatigue crack growth rates may range from a factor of 2 to 4 under identical loading conditions, these ratios are quite good.

REFERENCES

1. Barson, J. M.; and Rolfe, S. T.: Correlations Between K_{Ic} and Charpy V-Notch Test Results in the Transition Temperature Range. Impact Testing of Metals, ASTM STP 466, 1970, pp. 281-302.

2. Hudson, C. Michael: Effect of Stress Ratio on Fatigue Crack Growth in 7075-T6 and 2024-T3 Aluminum-Alloy Specimens. NASA TN D-5390, 1969.

3. Forman, R. G.; Kearney, V. E.; and Engle, R. M.: Transactions, American Society of Mechanical Engineers. Series D, J. of Basic Engineering, vol. 89, no. 3, Sept. 1967, pp. 459-464.

4. Hudson, C. M.; and Lewis, P. E.: NASA Langley Research Center's Participation in a Round-Robin Comparison Between Some Current Crack-Propagation Methods. Part-Through Crack Fatigue Life Prediction, J. B. Chang, ed., ASTM STP 687, 1979, pp. 113-128.

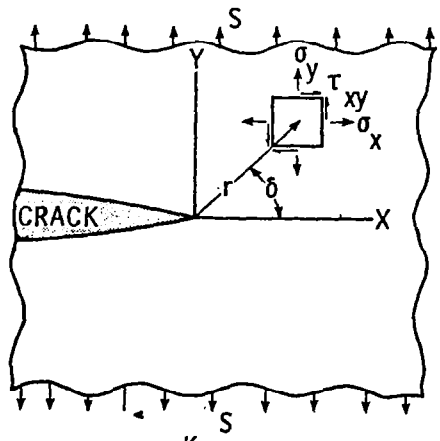

$$\sigma_y = \frac{K_I}{\sqrt{2\pi r}} f(\delta)$$

$$\sigma_x = \frac{K_I}{\sqrt{2\pi r}} g(\delta)$$

$$\tau_{xy} = \frac{K_I}{\sqrt{2\pi r}} h(\delta)$$

Figure 1.- Stress characterization in the vicinity of a crack tip.

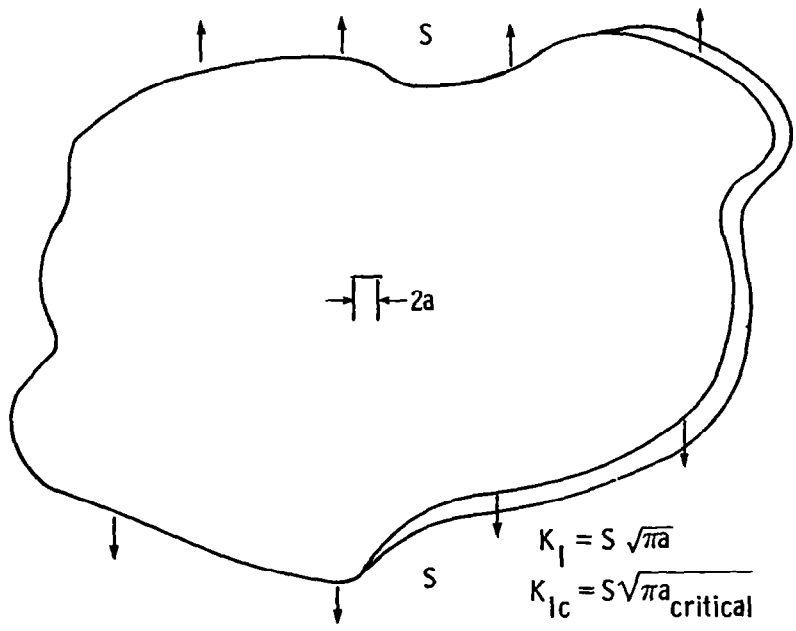

Figure 2.- Stress intensity solution for a through-the-thickness crack in an infinite-width plate.

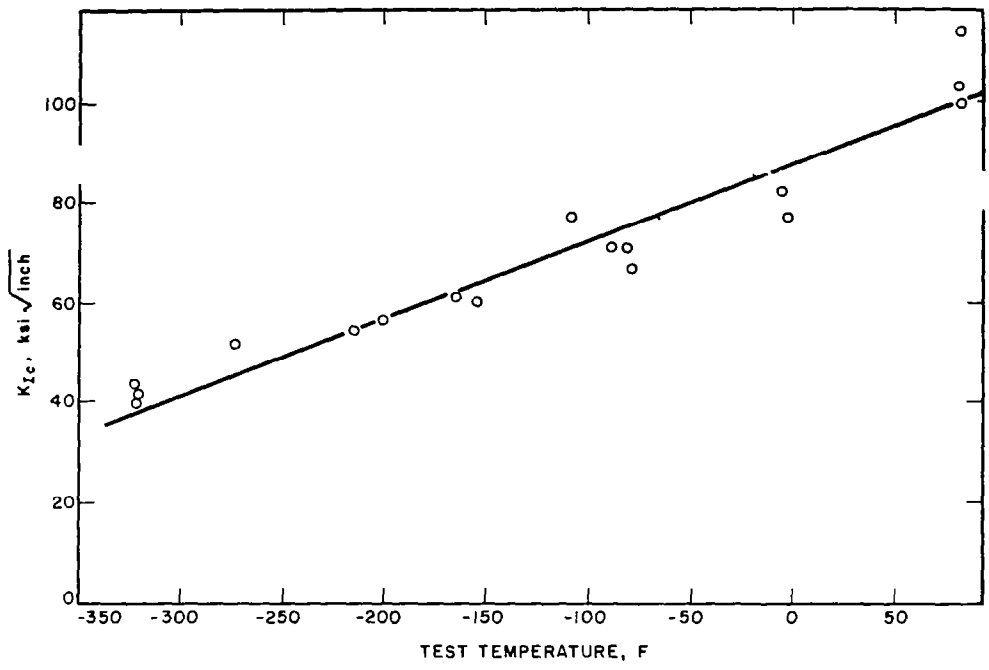

Figure 3.- Variation of K_{1c} with temperature for 18 Ni-(250) maraging steel. (From ref. 1.)

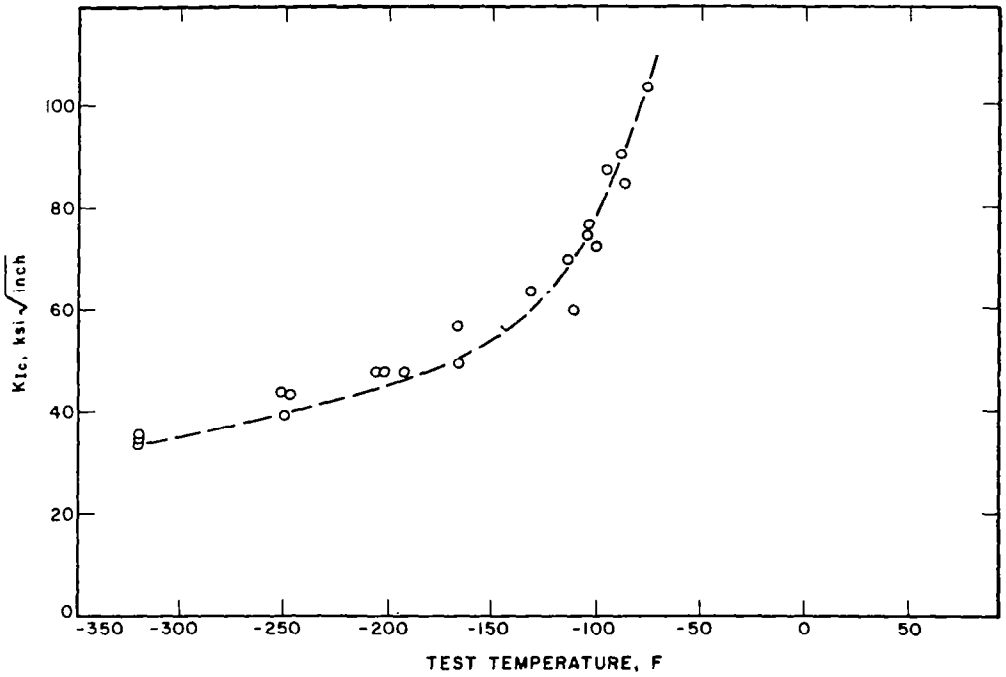

Figure 4.- Variation of K_{1c} with temperature for ASTM A517 Grade F steel. (From ref. 1.)

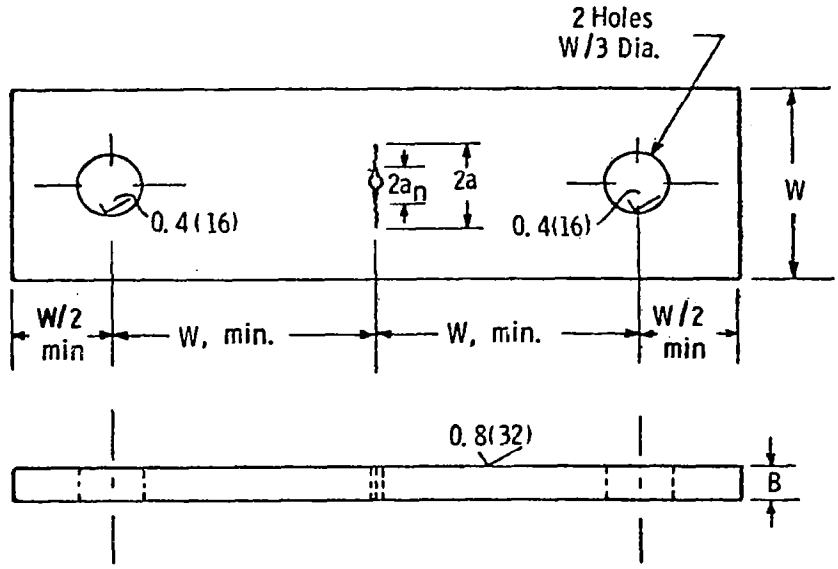

Figure 5.- Center-cracked tension specimen.

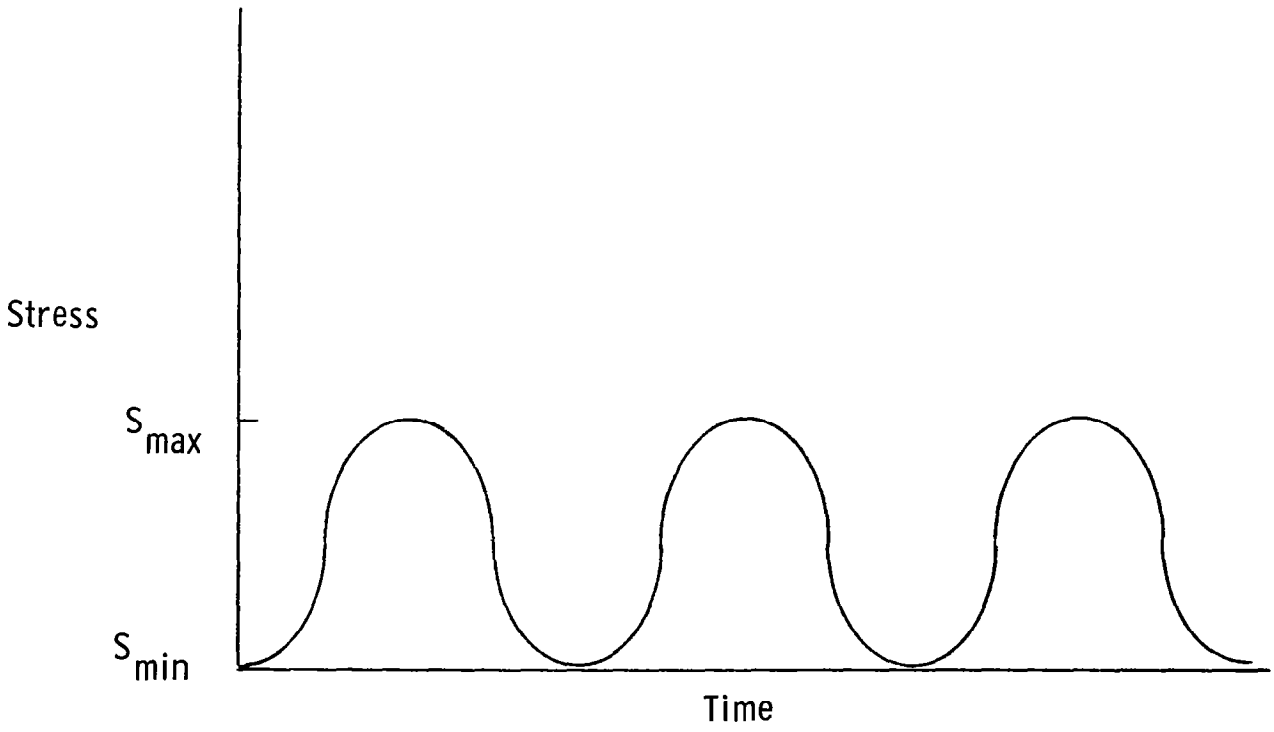

Figure 6.- Variation of stress with time.

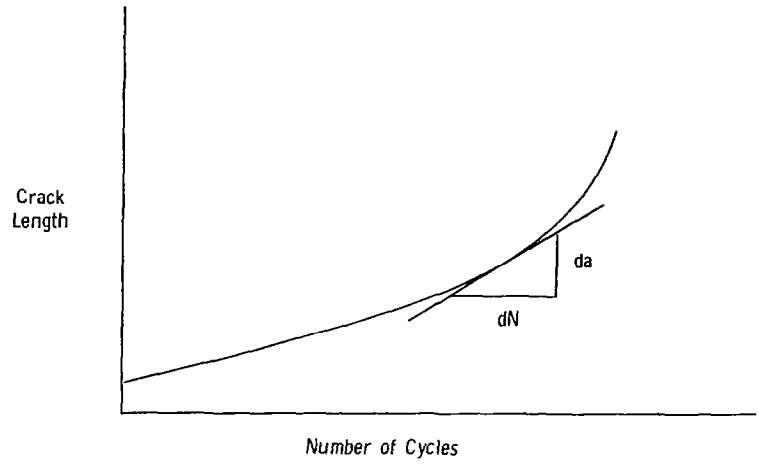

Figure 7.- Variation of crack length with number of cycles.

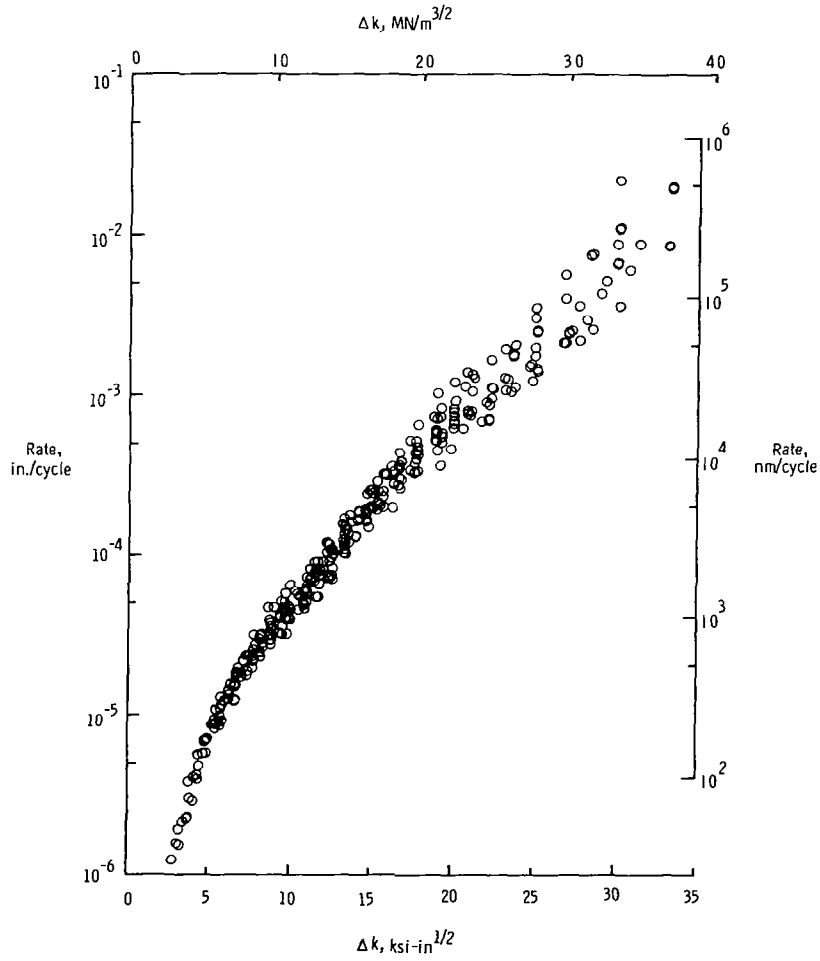

Figure 8.- Variation of da/dN with ΔK. (From ref. 2.)

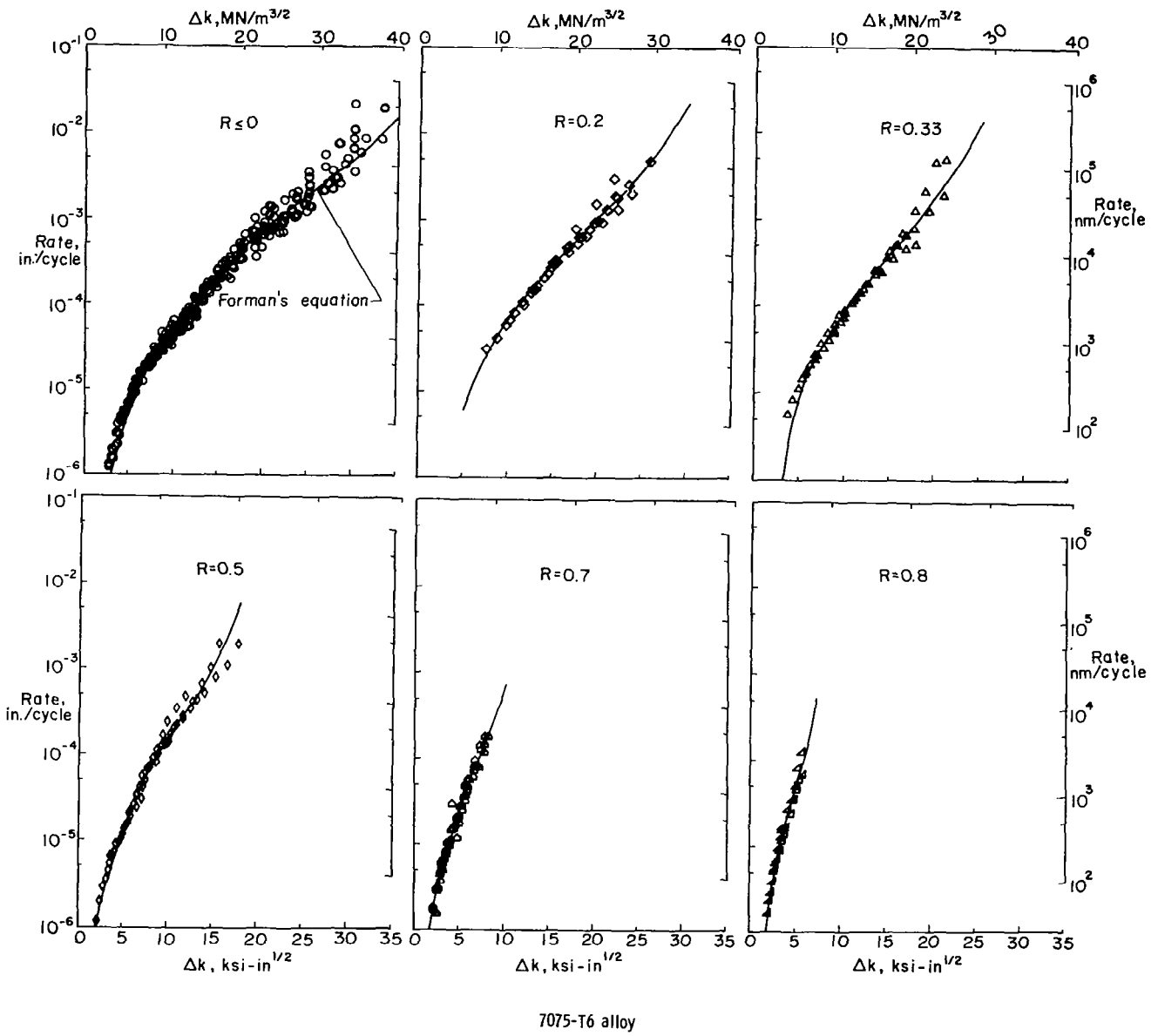

Figure 9.- Variation of da/dN with ΔK for various R values. (From ref. 2.)

SPECIMEN NUMBER	TEST LIVES/PREDICTED LIVES
23-10	1.00
23-12	1.19
23-13	1.03
23-14	1.05
23-16	0.65
23-17	0.60
23-18	1.26
23-76	0.51
37-2	1.84
37-3	0.70

Figure 10.- Ratios of test lives to predicted lives.